# Applications of Nuclear Quadrupole Interactions in Materials Research\*

Zhu Shengyun

China Institute of Atomic Energy, P. O. Box 275-50, Beijing 102413, P. R. China

Z. Naturforsch. **53 a,** 340–348 (1998); received February 25, 1998

The principle of the time differential perturbed angular correlation and distribution technique which measures the nuclear quadrupole interaction is briefly described. Some examples are given to show the possibilities of this technique in microscopic studies of materials.

#### 1. Introduction

The nuclear quadrupole interaction (NQI) is a hyperfine interaction between a nuclear quadrupole moment and an extranuclear electric field. The electric field gradients (EFG's) are directly connected to micro-structure of materials and any tiny change of nuclear environment can cause changes of the extranuclear EFG's, and hence nuclear quadrupole interactions. Therefore, the nuclear quadrupole interactions can be used to investigate on an atomic scale material properties such as micro-structure, electronic structure, magnetism, impurities and defects, etc.

There has been a variety of techniques to detect NQI's. Among them are Mössbauer effect (ME), nuclear magnetic and quadrupole resonances (NMR and NQR), nuclear orientation (NO), perturbed angular correlation and distribution (PAC and PAD), etc.

In this paper the PAC and PAD technique will be briefly introduced and some examples of its applications in materials research will be given. This technique has been known for about 40 years. Most early applications involved measuring nuclear moments. In the past twenty years it has been developed as a sensitive tool in condensed matter physics, with applications to a wide range of problems involving nuclear hyperfine interactions. Compared to ME, NMR and NQR and NO, the PAC and PAD technique has some advantages. ME is restricted to nuclear states which have excitation energies of less than 100 keV, to low

temperature in most cases and to solids, and the measured NOI is usually a superposition of the NOI and isomer shift. NMR and NQR needs large amounts of probe nuclei and has a skin effect which prevents the investigation of bulk metallic materials. NO is usually performed at very low temperature (mK range). In PAC and PAD studies useful information is provided by  $\gamma$  rays. Therefore, the PAC and PAD technique can be used to study all kinds of materials, such as gases, liquids and solids including metals, alloys, ceramics, semiconductors, superconductors, nanocrystalline materials, superlattices, amorphous solids, etc. The PAC and PAD measurements can be performed at any temperature and pressure with very small probe concentrations. The excited states of interest are not limited to low-lying excited states as in ME, but this technique can not be applied to the ground state.

# 2. Time Differential Perturbed Angular Correlation and Distribution

The time differential perturbed angular correlation technique (TDPAC) [1] makes use of the spin precession in excited nuclear states with a certain lifetime  $\tau$ , usually in the  $10^{-9}$  -  $10^{-6}$  sec range, and requires some degree of orientation of the precessing nuclei and some way to detect nuclear spin precession over the observed time interval. The principle of the TDPAC measurement is shown in Figure 1. The mother nucleus decays into the daughter probe nucleus of TDPAC. The intermediate excited state is populated by the emission of  $\gamma_1$ . The emitted  $\gamma_1$  is detected by a "start" detector. The detection of  $\gamma_1$  defines the time t=0 at which the nucleus decays to the intermediate excited state and, most importantly, selects a certain

Reprint requests to Prof. Zhu Shengyun; Fax: +86-10-69357787, E-mail: ciasyz@public.bta.net.cn.

<sup>\*</sup> Presented at the XIVth International Symposium on Nuclear Quadrupole Interactions, Pisa, Italy, July 20–25, 1997.

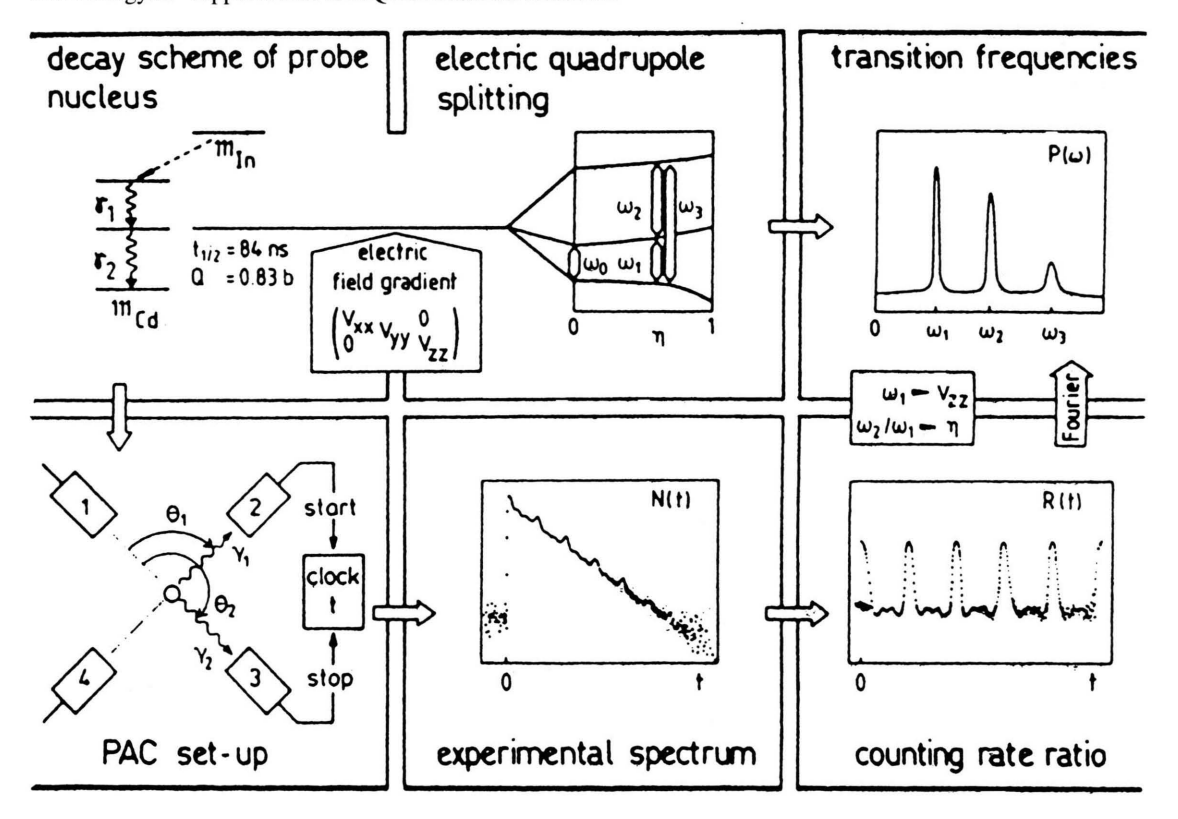


Fig. 1. Schematic of the experimental set-up in a TDPAC measurement.

set of nuclei having a higher probability of emitting  $\gamma_1$  and a certain direction at which nuclei with their angular momentum I are preferably aligned. The degree of the alignment is of the order of 10 - 50%. The intermediate excited state is de-excited to the ground state by the emission of  $\gamma_2$  which is detected by a "stop" detector. The detection of  $\gamma_2$  determines the spin precession.

If the excited state is subjected to perturbations during its lifetime  $\tau$ , the total  $\gamma_2$  intensity is modulated by  $W(\theta,t)$  as

$$I(\theta, t) = I_0 e - \frac{t}{\tau} W(\theta, t) + B. \tag{1}$$

 $W(\theta, t)$  is the perturbed angular correlation function

$$W(\theta, t) = 1 + \sum_{k} A_k G_k(t) P_k(\cos \theta), \tag{2}$$

where  $A_k$  is the anisotropy coefficient,  $P_k(\cos \theta)$  the Legendre polynomial and  $G_k(t)$  the perturbation factor determining the time variation of the perturbed

angular correlation. In general,  $A_2 \gg A_4$ , and for polycrystalline samples we have

$$G_2(t)_{\text{mag}} = f_0 + \sum_i f_i e^{-\sigma(i)t} \cos(2\omega_{L_i} t),$$
 (3)

$$G_2(t)_{\text{ele}} = \sum_{n} S_{2n} \left[ f_0 + \sum_{i} f_i e^{-n\sigma(i)t} \cos(n\omega_{0i}t) \right]$$
(4)

for the magnetic and quadrupole interaction, respectively. In (3) and (4) the summation runs over all perturbations,  $f_0$  is the unperturbed fraction of the probe nuclei,  $f_i$  the fraction associated with the  $i^{\text{th}}$  perturbation,  $\omega_{L_i}(\omega_{0i})$  the  $i^{\text{th}}$  magnetic (quadrupole) interaction frequency and  $\sigma_i$  the width of the  $i^{\text{th}}$  frequency distribution. If no extranuclear perturbation is present,  $G_2(t) = 1$  and the usual angular correlation is obtained.

The TDPAC measurements are usually performed by using a four-detector set-up as shown in Fig. 1, and four or eight coincidence time spectra are recorded simultaneously. In the data analysis, in order to enhance the oscillation and eliminate the nuclear lifetime and other factors such as the detector efficiency, etc., a spin rotation function is usually formed

$$R(t) = \frac{I(\theta_1, t) - I(\theta_2, t)}{I(\theta_1, t) + I(\theta_2, t)}.$$
 (5)

For the four-detector spectrometer we have

$$R(t) = \frac{\sqrt{I_{12}(\theta_1, t)I_{43}(\theta_1, t)} - \sqrt{I_{13}(\theta_2, t)I_{42}(\theta_2, t)}}{\sqrt{I_{12}(\theta_1, t)I_{43}(\theta_1, t)} + \sqrt{I_{13}(\theta_2, t)I_{42}(\theta_2, t)}},$$
(6)

assuming that the detectors 1 and 4 record  $\gamma_1$  and the detectors 2 and 3  $\gamma_2$ .  $\theta_1$  and  $\theta_2$  are symmetrically set at  $\pm 135^\circ$  or  $\pm 45^\circ$  for the magnetic case and at 90° and 180°, respectively, for the quadrupole case. The analytical expressions of R(t) for magnetic and quadrupole interactions can be easily deduced as

$$R(t)_{\rm mag} = \frac{3A_2}{4+A_2}G_2(t)_{\rm mag}$$
 and 
$$R(t)_{\rm ele} = \frac{3A_2}{4+A_2G_2(t)_{\rm ele}}G_2(t)_{\rm ele}.$$
 (7)

The hyperfine interaction parameters,  $A_2$ ,  $f_i$ ,  $\omega_{L_i}(\omega_{0i})$  and  $\sigma_i$ , can be obtained by fitting the experimentally measured R(t) with (7). From these parameters, information about material properties can be extracted. For example, structures and defects can be identified by the interaction frequency  $\omega_i$ , their fractions or concentrations are given by the fraction  $f_i$ , and the frequency distribution width can result in information on crystalline order and disorder.

There are more than 40 elements suitable for TD-PAC measurements. The best TDPAC isotopes are <sup>99</sup>Ru, <sup>100</sup>Rh, <sup>111</sup>Cd, <sup>117</sup>In, <sup>133</sup>Cs, <sup>140</sup>Ce, <sup>155</sup>Gd, <sup>181</sup>Ta, and <sup>204</sup>Pb, among which <sup>100</sup>Rh, <sup>111</sup>Cd, and <sup>181</sup>Ta are most frequently used. The TDPAC isotopes or probe nuclei are usually embedded into the samples in question by one of the following ways: alloying, diffusion, implantation, nuclear reaction and nuclear reaction recoil implantation.

For the TDPAD measurements no coincidence or "correlation" is required as in TDPAC. The excited states of interest are directly populated and aligned by the nuclear reaction. The time t=0 is fully defined by the beam pulse. The angular distribution precessing

in extranuclear fields is measured only as a function of time by two detectors at fixed angles.

Traditionally, a slow-fast coincidence system, in which the fast time signals are gated by the slow energy signals, is used in the TDPAC measurements [2]. We have developed a fast-fast coincidence TDPAC spectrometer containing four BaF<sub>2</sub> scintillation detectors [3], in which the slow energy signal gating is not adopted. Therefore, the dead time effect is greatly reduced, intense radioactive sources or high counting rates are allowed and the requirement for electronics stability is relaxed. We have also established a TDPAD spectrometer and an integral PAD(PAC) spectrometer composed of four BGO-Compton-suppressed HPGe detectors for excited states with lifetimes of  $10^{-9}$  -  $10^{-13}$  sec at the HI-13 tandem accelerator [4].

# 3. Applications of Nuclear Quadrupole Interactions in Materials Research

To show the possibilities of the TDPAC technique in microscopic studies of materials, some of its applications in materials research will be described with some experimental results obtained at the China Institute of Atomic Energy.

# 3.1. Defects and Radiation Damage

The investigation of defects and radiation damage in materials is a major field of TDPAC applications. Structural and dynamical defect aspects as well as identification of defects on an atomic scale are the main thrust of the TDPAC technique. We have investigated defects and radiation damage in many semiconductors and metals. Only two examples are given here.

# 3.1.1. Defects in <sup>178</sup>W Heavy Ion Irradiated Si [5]

The Si sample was recoil-implanted by  $^{178}$ W produced by the  $^{181}$ Ta (p,4n) nuclear reaction, and the  $^{178}$ Hf probe nuclei in it were created by the successive EC decays of  $^{178}$ W. The implantation fluence of  $^{178}$ W was  $5\times10^{11}$ /cm² which is equivalent to  $2.5\times10^{19}$ /cm² neutrons. The TDPAC measurements were performed on the 1.350 - 0.093 MeV, 2.2 ns cascade in  $^{178}$ Hf as a function of annealing temperature up to 800 °C. The data analysis yields three quadrupole interaction frequencies of  $\omega_{01} = 2002$  Mrad/s,  $\omega_{02} = 594$ 

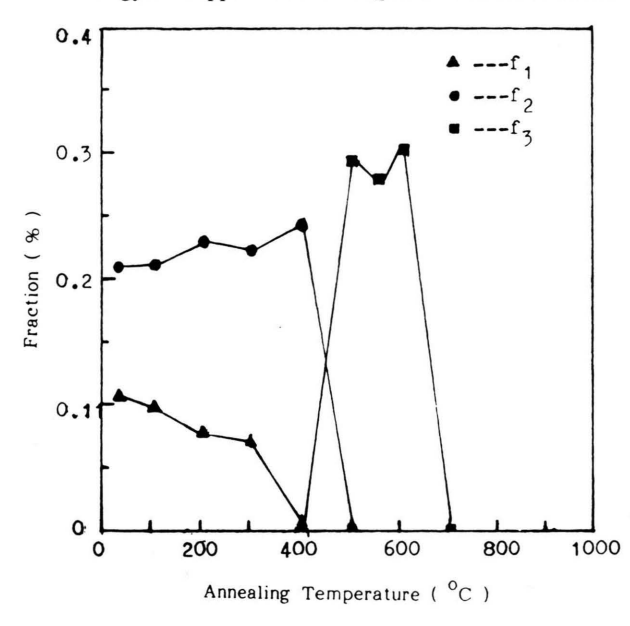


Fig. 2. Fractions  $f_i$  of <sup>178</sup>Hf probe atoms in heavy ion irradiated and annealed Si with V<sub>1</sub>-type defects  $(f_1)$ , V<sub>2</sub>-type defects  $(f_2)$  and V<sub>4</sub>-type defects  $(f_3)$ .

Mrad/s and  $\omega_{03}$  = 142 Mrad/s. The defects characterized by  $\omega_{01}$  are connected to the  $V_1$ -type defects, i. e. monovacancy-oxygen complex, by  $\omega_{02}$  to the  $V_2$ -type defects, i.e. divacancy and divacancy-oxygen complex and by  $\omega_{03}$  to the V<sub>4</sub>-type defects, i. e. quadrivacancy and quadrivacancy-oxygen complex. The fractions of the observed three defects are illustrated in Fig. 2 as a function of annealing temperature. The V<sub>1</sub>-type defects were observed from room temperature (RT) to 400 °C with a decreasing fraction  $f_1$ , the V<sub>2</sub>-type defects were detected up to 500 °C with a slowly increasing fraction  $f_2$  and the  $V_4$ -type defects are formed between 400 - 700 °C during annealing. These defects are annealed at 400 °C, 500 °C and 700 °C, respectively. The obtained results are confirmed by our positron annihilation measurements. This example shows that the TDPAC technique is able to identify and study very complex defects and defect dynamics in materials.

# 3.1.2. Radiation Damage in Ag [6]

The results of the radiation damage investigation in Ag are presented to show the sensitivity of this technique to defect studies. A unique quadrupole interaction with a sharp frequency of 76.2 Mrad/s was detected in Ag recoil-implanted by <sup>111</sup>In of 1 MeV

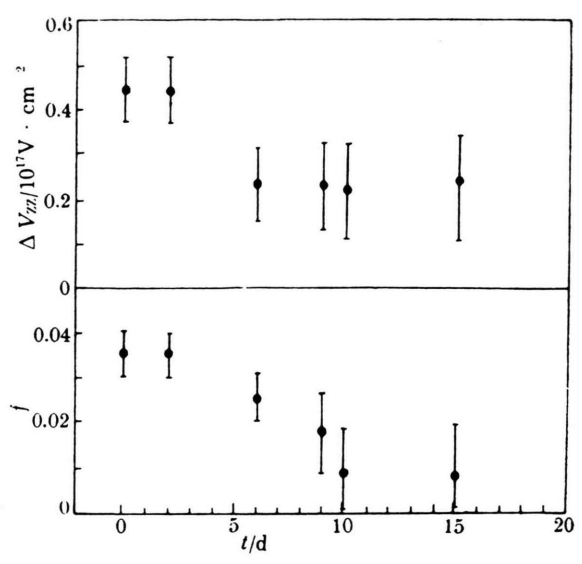


Fig. 3. Variation of relative fraction f and EFG distribution width  $\Delta V_{zz}$  with healing time.

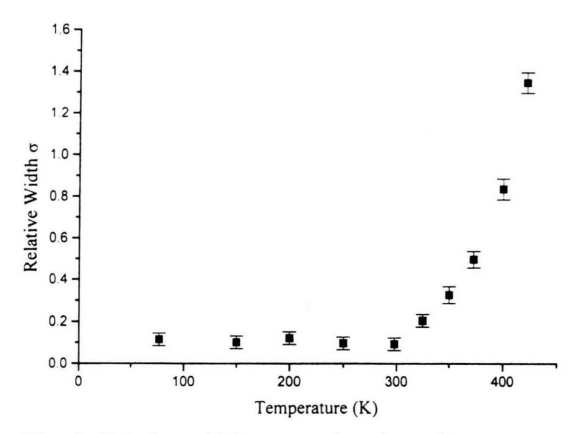


Fig. 4. Relative width  $\sigma$  as a function of temperature in  $In_{0.95}Ga_{0.005}Ag_{0.045}.$ 

and  $10^{14}$ /cm² from the reaction  $^{109}$ Ag  $(\alpha,2n)^{111}$ In, indicating that monovacancies were created in Ag by the recoils, the relative intensity of which is only  $\sim 3.5\%$ . After annealing at 673 K, the unique quadrupole interaction disappeared and the probe nuclei experienced just an interaction of the EFG distribution caused by distant defects. The radiation damage was completely annealed at 873 K. Figure 3 displays the dependence of the radiation damage on healing time at RT. It can be seen that the healing effect mainly takes place in 2 to 10 days after irradiation and the probe nuclei still trap defects after 15-day healing, but with a reduction of a factor of 3.5.

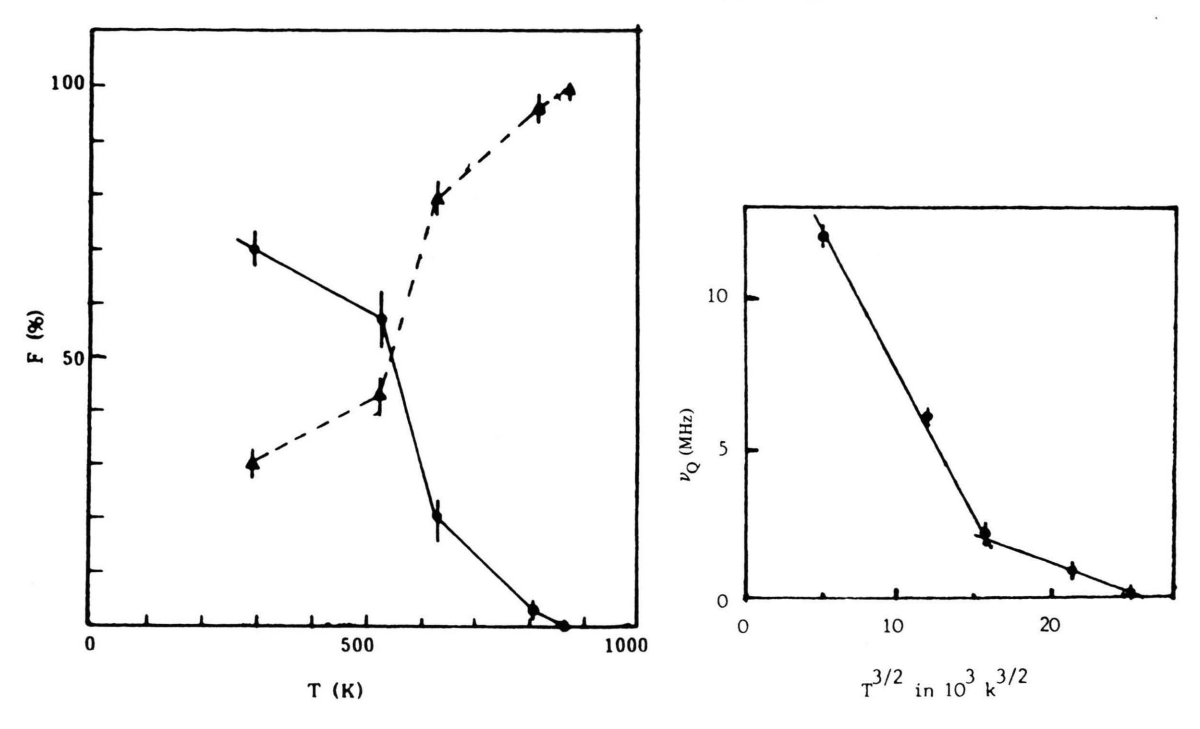


Fig. 5. Fractions  $f_1$  ( $\bullet$ ) and  $f_2$  ( $\blacktriangle$ ) of <sup>111</sup>Cd at the sites 1 and 2 as a function of temperature T in  $Pd_{0.80}Si_{0.20}$  (left) and  $T^{3/2}$  temperature dependence of the quadrupole interaction in  $Pd_{0.75}Si_{0.20}Ag_{0.05}$  (right).

#### 3.2. Order-disorder Transformation [7]

The temperature dependence of the nuclear quadrupole interactions of <sup>111</sup>Cd was determined in the ternary alloy In<sub>0.95</sub>Ga<sub>0.005</sub>Ag<sub>0.045</sub> by the TDPAC method from 77 to 422 K. The electric field gradients and their widths were derived. The EFG width is related to the degree of crystalline order. A well-ordered alloy gives rise to a unique EFG, otherwise an EFG with a certain distribution. The lower the degree of order, the larger the width. The temperature dependence of the derived EFG distribution width is shown in Fig. 4, which clearly demonstrates that this alloy undergoes an order-disorder transformation at RT. The alloy is well ordered below RT and disordered above RT. The degree of disorder increases with increasing temperature. This alloy is of great importance to electronic devices. The practical use of the devices made of it shows that their performances become worse with a temperature increase above RT. The present results give a vivid explanation of the performance worsening.

### 3.3. Structure and Phase Transition [8]

The intermetallic compounds Pd<sub>0.75</sub>Si<sub>0.20</sub>Ag<sub>0.05</sub> and Pd<sub>0.80</sub>Si<sub>0.20</sub> are very useful materials in industry. It has been shown that their macroscopic properties change drastically with temperature and two compounds exhibit much different properties. To understand it, the TDPAC studies were performed on them from RT to 870 K. The temperature dependence of the quadrupole interaction frequency  $\nu_0$  is drawn for  $Pd_{0.75}Si_{0.20}Ag_{0.05}$  in Fig. 5, which exhibits a  $^{3/2}T$ dependence with a coefficient  $B = 5.43 \times 10^{-5} \text{K}^{-3/2}$ and  $B = 3.70 \times 10^{-5} \text{K}^{-3/2}$  below and above 630 K, exhibiting a phase transition at around 630 K. In Pd<sub>0.80</sub>Si<sub>0.20</sub> two silicides, PdSi and Pd<sub>2</sub>Si, were observed and the EFGs connected to them do not change with temperature. But, their fractions vary severely with temperature, as shown in Figure 5. Below 520 K one silicide is dominant, while above 520 K the other is dominant, revealing a picture of phase transition between two silicides. The quadrupole interactions are much different and strongly depend on temperature

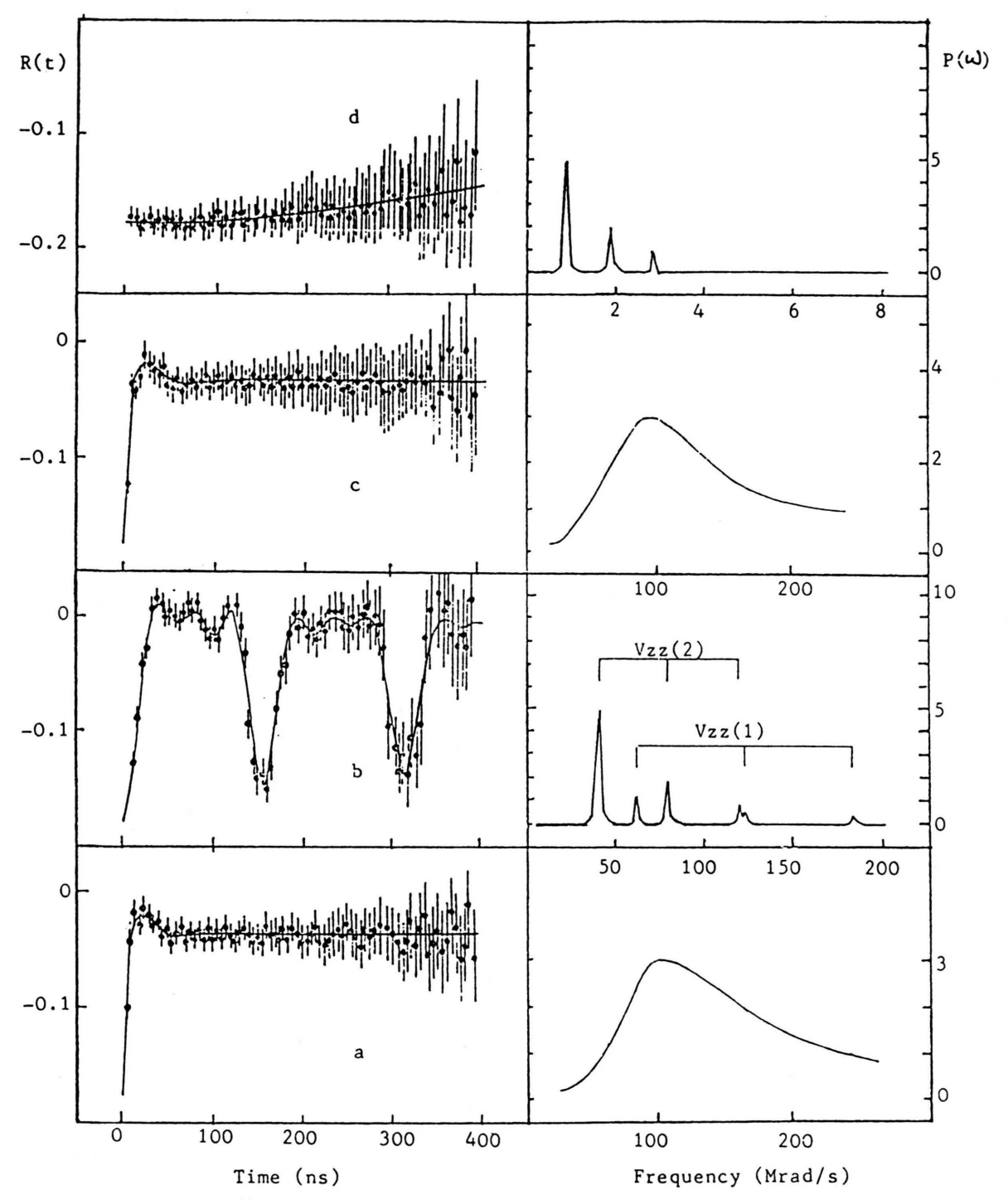


Fig. 6. TDPAC spectra of  $^{111}$ Cd in amorphous (a) and crystalline (b)  $Pd_{0.80}Si_{0.20}$ , and in amorphous (c) and crystalline (d)  $Pd_{0.75}Si_{0.20}Ag_{0.05}$  (left) and their corresponding quadrupole interaction frequency distribution (right).

in these two compounds. Thus, the present results can well explain why these two compounds show different properties and their macroscopic properties change with temperature. The present experiment illustrates that the quadrupole interaction investigation can help to establish the relationship between microand macro-properties of materials.

# 3.4. Crystalline Structure of Amorphous Alloys [9]

The quadrupole interactions in two amorphous alloys  $Pd_{0.75}Si_{0.20}Ag_{0.05}$  and  $Pd_{0.80}Si_{0.20}$  were investigated below and above the crystallization temperature  $T_{\rm crv}$ . As shown in Fig. 6, the broad EFG distributions with a width of 0.48 - 0.51 were sensed by the probe nuclei  $^{111}\mathrm{Cd}$  in them below  $T_{\mathrm{crv}}$ , and the unique quadrupole interaction frequencies were observed above  $T_{\rm crv}$ . The probe nuclei in different locations on an atomic scale feel different EFGs, and this spatial fluctuation of the EFGs causes a broad EFG distribution. The TDPAC technique measures the EFGs acting on the probe nuclei. Therefore, the measured EFGs can be directly compared with the EFGs calculated by different theoretical models, resulting in the origin of the broad EFG distribution. The present results are in good agreement with the computer simulation of the hard-sphere random packing model, i.e. the continuous random model. This confirms that the observed broad EFG distribution is caused by the continuous random structure, that is, short-range order and long-range disorder in amorphous materials.

# 3.5. High T<sub>c</sub> Superconductivity [10]

Our positron experiment pointed out that a charge transfer occurs at the superconduction transition temperature  $T_{\rm c}$  and there exists a normal state anomaly 20-30 K above  $T_{\rm c}$  in YBaCuO. To confirm the observed phenomena, the high  $T_{\rm c}$  superconductivity was investigated by the TDPAC technique between 77 K and RT. The same sample of YBaCuO with  $T_{\rm c}$  = 90 K as used in the positron annihilation study was employed, and the  $^{99}{\rm Mo}/^{99}{\rm Tc}$  probe nuclei were diffused into it. Figure 7 shows the temperature dependence of the EFG and its asymmetry parameter  $\eta$ , which is proportional to the crystallographic asymmetry  $\eta = 2(c-a)/(c+a)$ . Abrupt changes can be seen at the transition temperature  $T_{\rm c}$  and 125 K. The  $\eta$  values from 77 K to RT strongly suggest that a

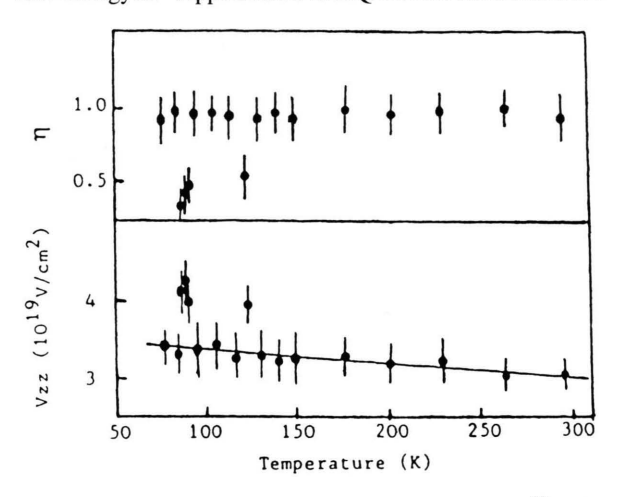


Fig. 7. Temperature dependence of  $V_{zz}$  and  $\eta$  for  $^{99}{\rm Tc}$  in YBa<sub>2</sub>Cu<sub>3</sub>O<sub>7-x</sub>.

transition of two- to one- dimensional Cu-O-Cu chain structure takes place during the superconduction transition. The one-dimensional Cu-O-Cu chain greatly favors a charge transfer from the CuO layer to the CuO chain in the high  $T_{\rm c}$  superconduction transition in YBaCuO. An anomaly of the normal state was clearly demonstrated around 125 K which is interpreted by a structural instability or phase softening.

# 3.6. Local Susceptibility [11]

The temperature dependence of the local susceptibility of Ce-impurity atoms in a La single crystal was measured with the TDPAC method from 6K to RT. The temperature dependence of the paramagnetic enhancement factor  $\beta$  and the anisotropy  $A_2$  are shown in Figure 8. They are clearly anomalous. For T > 50K it shows the  $T^{-1}$  behavior of a normal susceptibility. At 30 K it reaches a maximum and then drops rapidly. Below 10 K there is an almost T-independent region corresponding to a very low susceptibility. In the low temperature region (< 20 K) there is also an early loss of the anisotropy. Below 50 K the magnetic susceptibility departs from an ordinary Curie-Weiss law. This was observed by many groups and is interpreted as the Kondo effect by Mekata et al. [12] and the intermediate valence by Thiel et al. [13]. The present results detected a rapid reduction of the local susceptibility below 20 K, which is accompanied by a loss of anisotropy of the TDPAC signals. This may change the above interpretations. The loss of the anisotropy is not caused by the "after effect" in metals.

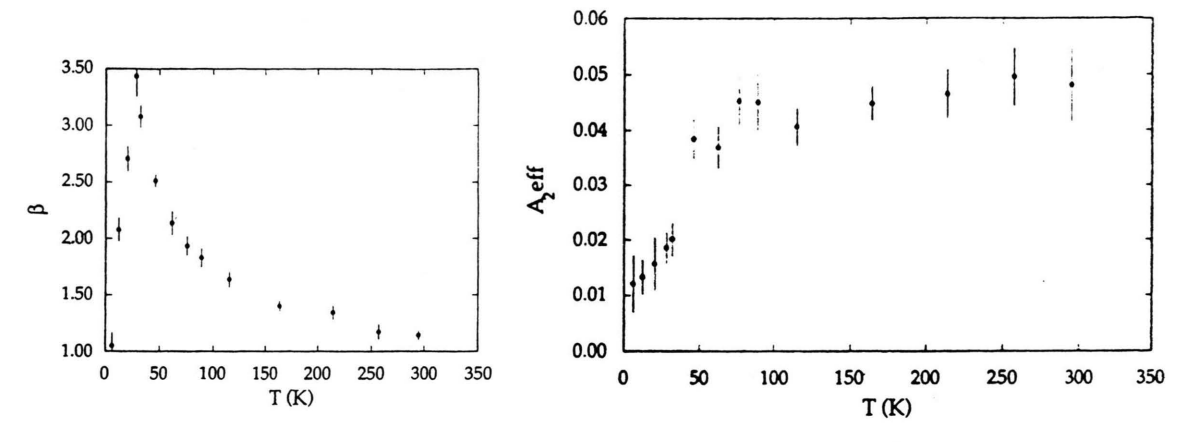


Fig. 8. Temperature dependence of paramagnetic enhancement factor  $\beta$  and anisotropy  $A_{\text{2eff}}$  for Ce in La.

This loss of anisotropy might be introduced by a very strong perturbation from a hyperfine field of  $\sim 90$  T at < 1 ns. Such a strong hyperfine field could be generated by the so called two-step process, that is, Ce ions continuously pick up and give a 4f electron to the conduction band, resulting in valence fluctuations.

#### 4. Conclusions

The TDPAC and TDPAD technique is a very sensitive and powerful tool in materials research. It can investigate phenomena in condensed matter and give information on material properties on an atomic scale. This technique will continue to play important roles in condensed matter physics in future. The main research fields of interest in the near future may involve: 1) Microstructure: This technique can be applied to investigate microstructures in both bulk materials and thin films, and help to establish the relationship

between the microstructure and macroscopic properties which can provide criteria for improving macroscopic properties of materials. 2) Defects and radiation damage: Point defects, dislocations, stacking faults, defect clusters and voids can be investigated microscopically not only in bulk materials but also in thin films, surfaces and interfaces. 3) Surface and interface: The study of surfaces and interfaces is one of the interesting topics in condensed matter physics. Surface magnetic and electronic structures, surface diffusion, surface roughening, surface defects, etc. can be investigated with a resolution of one atomic layer. 4) Magnetism: Hyperfine magnetic fields, local moments and magnetic structures can be determined on an atomic scale and 5) New materials: Microscopic investigations are increasingly demanded to develop high-quality new materials.

The author would like to express his heartfelt thanks to the colleagues for their participating in and making efforts to the above experiments.

- R. M. Steffen and H. Frauenfelder, in Perturbed Angular Correlation edited by E. Karlsson, E. Matthias, and K. Siegbahn, North-Holland Publishing Company, Amsterdam (1964).
- [2] A. R. Arends, C. Hohenemser, F. Pleiter, H. De Waard, and R. M. Suter, Hyperfine Interactions 8, 191 (1980).
- [3] S. Y. Zhu, Q. Luo, Z. G. Fan, A. L. Li, Z. H. Gou, and S. N. Zheng, to be published in Nuclear Science and Techniques.
- [4] S. Y. Zhu, Q. Luo, Z. G. Fan, Z. H. Gou, S. N. Zheng, A. L. Li, G. S. Li, S. X. Wen, X. A. Liu, Z. Y. Dai, and X. G. Wu, to be published in Nuclear Science and Techniques.
- [5] Zhu Shengyun, Li Anli, Li Donghong, Huang Hanchen, Zheng Shengnan, Du Hongshan, Ding Honglin, Gou Zhenhui, and T. Iwata, Mater. Sci. Forum 175 - 178, 609 (1995).
- [6] Zhu Shengyun, Zuo Tao, and Li Donghong, Nucl. Tech. 16, 465 (1993).

- [7] Zhu Shengyun, Dong Minli, and Shen Weiqi, Hyperfine Interactions **30**, 283 (1986).
- [8] Zhu Shengyun, Zuo Tao, and Dong Minli, Hyperfine Interactions 39, 17 (1988).
- [9] Zhu Shengyun and Zuo Tao, Hyperfine Interactions **52**, 379 (1989).
- [10] Shengyun Zhu, Anli Li, Shengnan Zheng, Hanchen Huang, Donghong Li, Honglin Ding, Hongshan Du,
- and Hancheng Sun, Hyperfine Interactions **79**, 857 (1993).
- [11] E. Karlsson, B. Lindgren, M. Pan, M. Semple, and S. Y. Zhu, Hyperfine Interactions **78**, 559 (1993).
- [12] M. Mekata, Y. Kano, M. Moriya, K. Tsuji, and T. Haseda, J. Phys. Soc. Japan 41, 1918 (1976).
- [13] T. Thiel, M. Bottcher, and E. Gerdau, Hyperfine Interactions **36**, 65 (1987)